JOURNAL OF SOLID STATE CHEMISTRY 102, 557–561 (1993)

BRIEF COMMUNICATIONS

Proton Conduction of MLaNb$_2$O$_7$ (M = K,Na,H) with a Layered Perovskite Structure

M. SATO,* T. JIN, AND K. UEMATSU

Department of Material and Chemical Engineering, Faculty of Engineering, Niigata University, Niigata 950-21, Japan

Received April 21, 1992; in revised form July 13, 1992; accepted July 15, 1992

The conductivities of the perovskite layered compounds $KLaNb_{12}O_7$ and its ion-exchanged forms $MLaNb_2O_7 \cdot xH_2O$ (M = Na,H) were investigated in the temperature range 20 to 80°C by complex impedance measurement with the samples held at various water vapor pressures. The conductivity for all the compounds obeyed the relationship $\sigma \propto P_{H_2O}^{1/n}$, although the $KLaNb_2O_7$ compound has no hydrous form. This fact suggested the possibility of proton conduction through the surfaces of particles. © 1993 Academic Press, Inc.

Introduction

In general, solid state proton conductivity in hydrates can be classified into two categories; i.e., bulk conductivity due to water of crystallization and surface conductivity due to water of adsorption. In particular, surfaces and intergranular contacts of particles within polycrystalline specimens take part in proton conduction (*1, 2*). The layered acid hydrates, such as H-montmorillonite (*3*) and α-$Zr(HPO_4)_2 \cdot H_2O$ (*4*), exhibit high proton conductivities along the hydrated surfaces of the microcrystals.

Recently the new layered acid hydrate $HLaNb_2O_7 \cdot xH_2O$ was prepared by the ion-exchange reaction of $KLaNb_2O_7$ with HNO_3 solution (*5*). Since this compound can be regarded as another example of a layered acid hydrate, we have, in this study, investigated the anticipated proton conductivity under various water vapor pressures. For comparison, the conductivities of $KLaNb_2O_7$ and $NaLaNb_2O_7 \cdot xH_2O$ were also investigated.

Experimental

$KLaNb_2O_7$ was prepared by solid state reaction of K_2CO_3, La_2O_3, and Nb_2O_5 powders. Thoroughly mixed starting materials with appropriate amounts of these powders were fired at 1240°C in air for 3 hr. An additional 25 mol% of K_2CO_3 was added in excess to avoid a possible loss of potassium due to volatilization. The above firings were carried out with two intermittent grindings to ensure efficient mixing of the reactants so as to yield monophasic products. The product was washed thoroughly with dis-

* To whom correspondence should be addressed.

0022-4596/93 $5.00

tilled water to wash away the excess potassium ions. Ion-exchanged forms, $NaLaNb_2O_7$ and $HLaNb_2O_7$, were obtained by reacting $KLaNb_2O_7$ powder with $NaNO_3$ molten salts at 400°C for 24 hr and with 6 *M* HNO_3 solution at 60°C for 24 hr, respectively. All the ion-exchanged products obtained were washed with distilled water and dried at 30°C. The completion of the ion-exchange reaction was confirmed by X-ray powder diffraction (XRD) and X-ray fluorescence analyses. Before measurements of thermogravimetric analysis (TGA) and conductivity, all the samples were preequilibrated at the water vapor pressure of 3.16 kPa (equal to the water vapor pressure at 25°C).

The measurements of XRD were done by using a Rigaku RAD-rA diffractometer equipped with a high temperature furnace attachment. The Cu$K\alpha$ radiation used was monochromatized by curved-crystal graphite.

The thermal stability and the amount of hydration for the products were examined by thermogravimetric analysis (TGA) with a Mac Science thermal analyzer system 001.

Specimens were prepared for conductivity measurement by pressing the powder sample into a compact disc at a pressure of 400 kg cm^{-2}. The disc was of typical dimensions 10 mm diameter and about 1.0 mm thickness, and its two opposite sides were coated with an evaporated Au film. The conductivities were determined from complex impedance diagrams obtained using alternating currents with frequencies between 40 Hz and 100 kHz, using a Hioki 3520 Hi Tester in the temperature range 20–80°C under various water vapor pressures. These conditions were achieved by streaming air, saturated with water vapor by bubbling into distilled water held at various temperatures (0 to 90°C), through the measurement cell.

Results and Discussion

The $KLaNb_2O_7$ structure consists of $LaNb_2O_7$ perovskite double layers, joined by corner sharing between the NbO_6 octahedra (*6*). The potassium ions, which are surrounded by six oxygen atoms with trigonal prismatic coordination, are situated between the perovskite layers. The structure of the anhydrous Na and H forms is basically the same as that of $KLaNb_2O_7$, but the stacking of the perovskite layers is somewhat different (*7*).

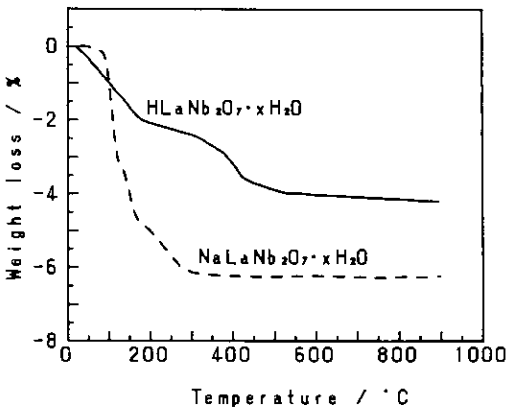

FIG. 1. TGA curves for $HLaNb_2O_7 \cdot xH_2O$ and $NaLaNb_2O_7 \cdot xH_2O$ preequilibrated with a water vapor pressure of 3.16 kPa at 25°C.

The Na- and H-exchanged compounds were always obtained in a hydrous form after the ion-exchange product was washed with distilled water, while $KLaNb_2O_7$ has no hydrous form even after any treatments. Figure 1 shows the TGA curves for hydrous $NaLaNb_2O_7$ and $HLaNb_2O_7$. It can be seen that the H-form began losing weight as soon as the temperature was raised above room temperature, while the Na-form exhibits no weight loss below 80°C. At the temperature range from 180 to 300°C, a plateau-like region appeared for the TGA curve of the H form. High temperature XRD analysis showed the presence of anhydrous $HLaNb_2O_7$ in this temperature range, and showed some complex thermal decomposition products at temperatures higher than 300°C. From the total weight loss after heating to 900°C, the maximum hydrous form

equilibrated in 100% relative humidity at 25°C was found to be in agreement with the formula $HLaNb_2O_7 \cdot 0.5H_2O$. The indexing of the XRD patterns gave tetragonal systems with the lattice constants $a = 3.888$ Å and $c = 10.548$ Å for the anhydrous form and with $a = 3.890$ Å and $c = 11.404$ Å for the hydrous form, indicating that some water molecules in the hydrous form are located between the perovskite layers. Rietveld analysis for this compound failed to yield a meaningful assignment of water molecules to definite crystallographic sites. Therefore, the water molecules in the H form could have some zeolitic water character. This may be supported by the dehydration behavior observed in the TGA curve; e.g., the gradual weight loss in the temperature range from room temperature to 180°C. On the other hand, the TGA curve for the Na form clearly shows three dehydration steps at 80, 120, and 250°C, in which sharp endothermic peaks were observed in the DTA curve. The weight losses at 80, 120, and 250°C correspond, respectively, to the loss of 0.7, 1.0, and 1.6 mole of water, indicating the following sequence;

$$NaLaNb_2O_7 \cdot 1.6H_2O \xrightarrow{80°C} NaLaNb_2O_7 \cdot 0.9H_2O \xrightarrow{120°C} NaLaNb_2O_7 \cdot 0.6H_2O \xrightarrow{250°C} NaLaNb_2O_7 \xrightarrow{900°C} \text{oxides}.$$

The Rietveld analysis for the fully hydrated Na form indicates the location of water molecules in two crystallographic sites between the perovskite layers, the details of which will be reported elsewhere (*7*). The hydrating water molecules in the Na form seems to have the character of water of crystallization.

The data collection for the impedance measurement was done after the specimen reached its equilibrium for a given water vapor pressure. A typical ac-impedance diagram is shown in Fig. 2 for the hydrous H form. The diagram consists of part of a semicircle terminated with a sloping line. The same type of diagram was obtained for all other samples. The conductivity was determined from the low-frequency intercept of the semicircle by means of a nonlinear least-squares method. The frequency at the top of the semicircle in Fig. 2 (3.5 kHz) corresponds to a parallel capacitance of 1.3×10^{-10} F, which is greater by several orders of magnitude than the shunt capacity of the measuring cell. Both this large parallel capacity and the very depressed semicircle shown in Fig. 2 imply that the grain boundary participates in the conduction (*8*). In such a case, since the total grain boundary capacitance results from the sum of a series of individual boundaries, the measured capacitance is usually much larger than the cell shunt capacitance. Thus, two distinct semicircles can be seen in the impedance plots, although in our case the circle with low frequencies could not be distinguished

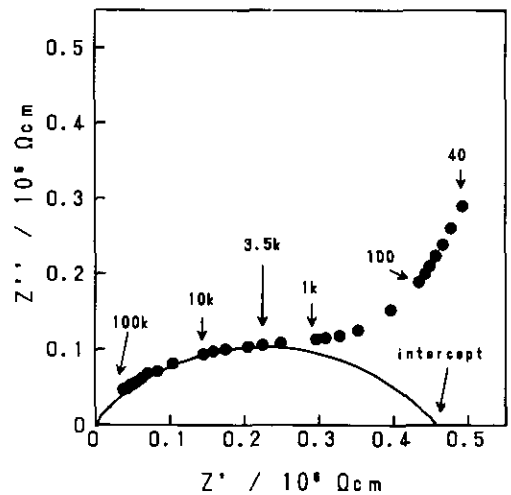

FIG. 2. Impedance diagram obtained at 25°C for $HLaNb_2O_7 \cdot xH_2O$ held under a water vapor pressure of 0.62 kPa. The solid line was calculated by a nonlinear least squares method using the data from 3 kHz to 100 kHz. Z' and Z'' mean the real and imaginary components of the impedance, respectively.

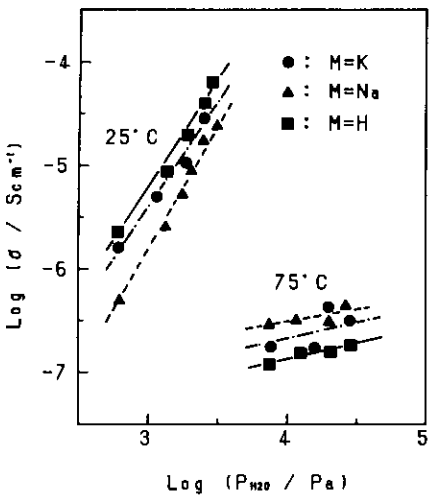

FIG. 3. Relationship between conductivity and water vapor pressure for $MLaNb_2O_7 \cdot xH_2O$ (M = K,Na,H).

from the circle with high frequencies, probably because of the small difference between the time constants for bulk and boundary components. Figure 3 shows the relationship between the conductivity and the water vapor pressure for all the compounds. An almost linear correlation can be seen in the log σ vs. log P_{H_2O} points for every sample. It has already been established that ionic conductivity through alkali ions and protons located between the perovskite layers occurs for temperatures higher than 300°C (*7*). This fact together with the essentially equivalent behavior found for all the samples shown in Fig. 3 indicates that the conductivity observed in wet atmospheres at near room temperature is attributable to proton conduction. It is also interesting that the $KLaNb_2O_7$ compound exhibited the same conducting behavior as those for other hydrous compounds although it has no hydrous form even under a wet atmosphere. Therefore, a large part of the proton conductivity observed in Fig. 3 is probably due to surface conduction along the grain boundaries, although the bulk conductivity could, of course, participate in the conduction to some extent. The linear correlation as shown in Fig. 3 leads to the equation

$$\sigma_p \propto P_{H_2O}^{1/n},$$

where σ_p is the proton conductivity and n is the constant depending on a given temperature. The values of n calculated by the least-squares method are around 2 at 25°C, around 10 at 50°C (data not shown), and around 50 at 75°C for all the samples. If the proton conductivity is proportional to the amount of the water adsorbed on the specimen, Eq. (1) leads to the equation of the well known Freundlich-type isotherm. The value of n for a Freundlich-type isotherm is usually greater than unity, and, roughly speaking, the value $1/n$ expresses the density of adsorption on a heterogeneous surface (*9*). That is, the proton conduction in the present case is likely to occur to some extent through the water molecules in the adsorption layer on the particle surface. Since such water molecules seems to be physically adsorbed, heating to above 100°C apparently removes most of the surface water, thereby removing the conduction medium. This situation as it typically occurs is shown in Fig. 4 for an $HLaNb_2O_7 \cdot xH_2O$ sample held under constant water vapor pressure above 35°C. The increase in the conductivity as the temperature increases from 25 to 35°C seems to indicate that some thermal activation processes are involved in the proton conduction. At present, it is not entirely clear why the surface proton conduction in the $MLaNb_2O_7$ compounds is more predominant than the bulk conduction through the interlayer water molecules. The ion-exchanged compounds of the Na and H forms are, however, extremely fine powders after the ion-exchange reaction. Therefore, the proton conduction might be similar to that for the $Nb_2O_5 \cdot xH_2O$ oxides, which consist of irregular amphoteric charged particles separated by an aqueous solution (*10*).

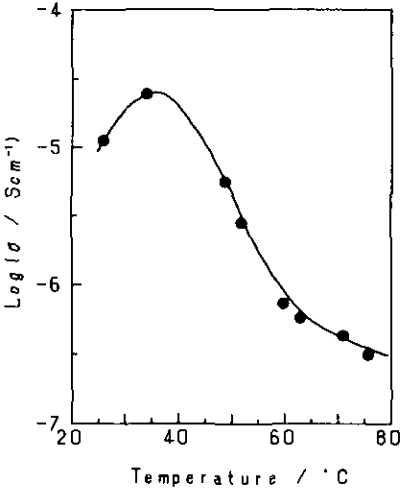

FIG. 4. Temperature dependence of conductivity for $HLaNb_2O_7 \cdot xH_2O$ held under a constant water vapor pressure of 3.16 kPa.

Further study, which is needed to clarify the conduction mechanism by measurements of pore distribution, surface area, and adsorption water, is currently being carried out.

References

1. W. A. ENGLAND, M. G. CROSS, A. HAMMETT, P. J. WISEMAN, AND J. B. GOODENOUGH, *Solid State Ionics* **1,** 231 (1980).
2. Y. WING, M. LAL, AND A. T. HOWE, *Mater. Res. Bull.* **15,** 1649 (1980).
3. S. H. SHEFFIELD AND A. T. HOWE, *Mater. Res. Bull.* **14,** 929 (1979).
4. M. CASCIOLA AND D. BIANCHI, *Solid State Ionics* **17,** 287 (1985).
5. J. GOPALAKRISHNAN, V. BHAT, AND B. RAVEAUE, *Mater. Res. Bull.* **22,** 413 (1987).
6. M. SATO, J. ABO, T. JIN, AND M. OHTA, *Solid State Ionics* **51,** 85 (1992).
7. M. SATO, J. ABO, T. JIN, AND M. OHTA, *J. Alloys Comp.* [formerly *J. Less-Common Met.*], in press.
8. R. D. ARMSTRONG, T. DICKINSON, AND P. M. WILLIS, *J. Elecroanal. Chem.* **53,** 389 (1974).
9. A. W. ADAMSON, *in* "Physical Chemistry of Surfaces," 2nd ed., p. 401, Wiley, New York (1967).
10. R. C. T. SLADE, J. BARKER, AND T. K. HALSTEAD, *Solid State Ionics* **24,** 147 (1987).